POLITECNICO
MILANO 1863

SCUOLA DI INGEGNERIA INDUSTRIALE
E DELL'INFORMAZIONE

Investigation of flashing induced oscillations in vertical two-phase flows near saturation conditions

Tesi di Laurea Magistrale in
Energy Engineering - Ingegneria Energetica

Karim Mohammed Abdalwaged Yassin, 10814553

Advisor:
Prof. Luigi Colombo

Co-advisors:
Prof. Carlos Dorao

Academic year:
2022-2023

Abstract: Two phase flow instability experiments were investigated in a forced circulation loop under low heating power and low pressure conditions. The observed instability was flashing induced and the oscillations took three main shapes, irregular intermittent oscillation, pure sinusoidal oscillation, and intermittent oscillation. The characteristics of the oscillating waves were analyzed based on the results of the mass flux, and fluid temperature. The effects of the pump bypass valve, the system pressure and the heating power on the oscillations amplitude, shape and frequency were investigated as well. It was found that the flashing is suppressed at high pressures and high powers, while intense oscillations occurred at low heat flux and low pressure.

Key-words: Forced circulation, Flashing, Flow instability, Boiling

1. Introduction

1.1. Introduction

New generating capacity is needed around the world to fulfill rising energy demand in many nations as well as to replace outdated fossil fuel units, particularly coal-fired ones that produce large amounts of carbon dioxide. Nuclear power will play a key role since it is the only low-carbon energy source that is dependable, scalable, and proven. At the moment, there are approximately 440 operating reactors, and about 60 under construction, which in total are providing 10% of the world's electricity [2]. Boiling water reactors (BWR) comes in second place after pressurized water reactors (PWR) as the most common nuclear reactors worldwide.
BWR is basically a two-phase flow system where the fluid is heated up by the nuclear core and the steam is separated to run a turbine, similar to an ordinary steam power plant with the difference of the heating source. The steam void content resembles an inherent safety issue especially at the start-up procedure of the plant; a transient power increase will level up the steam void, which lowers reactivity and power, hence limiting the excursions. For example, On March 9, 1988, LaSalle unit 2 suffered from oscillations in the power caused by trip of the re-circulation pumps during natural circulation [5]. The sudden decrease in feed-water flow rate initiated a series of self-sustained oscillations of the power with an amplitude of 25% rated power peak to peak and period of 2 to 3 seconds. Within 7 minutes the reactor shut down automatically due to the neutron high flux. Post-analysis revealed that, by the time of the scram, the oscillations were 100% peak to peak. The oscillations magnitude and change in power peak values were unpredictable based on past operating experiences.

Another incident was recorded on August 15, 1992, when Washington Nuclear Power unit 2 witnessed power oscillations during startup [6]. Review showed that the power was oscillating with 25% rated power peak-to-peak amplitude under 2 seconds period. Within 1 minute the magnitude reached 100% rated power and became self-sustained for another minute before scram. The cause of instability was later blamed on the poor distribution of core power caused by the control rod pattern, and the speed shift of the recirculation pump to move from startup to full power operation. The earliest review of two-phase flow instabilities was conducted by Boure et al. [3]: it showed that water-cooled reactors, among other systems, are subject to thermal-hydraulic instabilities triggered by small fluctuations in the flow (due to turbulences, flow pattern, or nucleation). These instabilities can cause disastrous phenomena such as boiling crises, thermal fatigue, and mechanical failure. Boure classified the instabilities based on their behavior and what triggers them. Generally, the onset of static instabilities is predictable by the steady state laws, and the flow ends up either stable at a different steady point or suffers a periodic behavior. Ledinegg instability is one example, where the flow experiences a sudden excursion to a new stable condition. On the other hand, dynamic instabilities, such as density wave oscillations, are the result of the interaction between flow forces (e.g., friction and buoyancy) and feedback mechanisms (e.g., void generation rate, pressure drop, enthalpy propagation). Furthermore, Boure clarified that some instabilities are the result of an interaction between several elementary mechanisms and are called compound instabilities. He also mentioned the pioneer work to analyze the thermal-hydraulic instabilities in BWR, naming it BWR instability. Fukuda [7] classified the Density Wave Oscillations (DWO) into type I and type II, where type I takes place around saturation condition and type II happens at high steam quality at the heater exit. When it comes to driving forces acting in the riser, gravitational pressure drop is dominant in type I, while frictional pressure drop is dominant in type II DWO. He further classified type I oscillation based on the circulation type (forced or natural) showing that forced circulation instability has a longer incubation time i.e., longer period. The variety and complexity of the thermal-hydraulic instability validates the persistent work of earlier researchers and highlights the significance of a thorough comprehension of the instability phenomena in nuclear reactor systems.

1.2. Literature Review

Flashing-induced oscillations were first investigated by Wissler et al. (1956) [16]. where they developed a simple model to find out the conditions under which self-sustained oscillations take place. They figured that to have oscillatory flow rate, the driving force in the rise must be greater than the frictional resistance to the flow. The oscillations have a period about the same value of the residence time of the fluid in the heater and the vertical rise, this is why it has been classified as type I DWO. Finally, they related the frequency and amplitude of the oscillations to the input heating power. It was not until the 90s that further experimental work revealed more information about flashing instabilities. Aritomi et al. [1] found that as the mass flux and the inlet temperature increase, the BWR during start-up can experience three different types of instabilities: geysering, flashing, and DWO. Jiang et al. [9] Provided the first detailed investigation on flashing related instabilities as well as a clear distinction between the two phenomena of flashing and geysering. While geysering is related to vapor generation, in the heating section, growth, detachment and condensation, the cause of vapor generation in flashing is the drop in hydrostatic head in the riser as the flow moves upward. Furthermore, they explained that the temperature of the fluid at the inlet of the riser must be greater than the saturation temperature at its exit for the flashing to occur. They assured that flashing-induced instabilities will occur during the start-up of natural circulation nuclear reactor, for pressure equal to atmospheric and higher. Manera et al. [11] Performed stability analysis for a CIRCUS facility, a full-height scaled steam/water loop of a natural circulation cooled BWR, under low pressure and low heating power conditions at a constant inlet subcooling. It was concluded that flashing is the main source of instability during start-up, and by increasing the power, the flow moves from stable single phase to stable two-phase passing by an instability region. There was no more room for doubt about how serious flashing instability is when it comes to the start-up of BWR, which lead to further research to have a better idea about the nature of the oscillations, their forms, characteristics, and how they can be avoided or alleviated. Natural circulation BWR (NCBWR) has been the topic of research for than three decades. It was proposed as a way to eliminate the use of recirculation pumps, hence avoiding pump trips that was thought to be one reason for instabilities in BWRs. In 1991 Aritomi [1] weighed the advantages and disadvantages of removing the recirculation pump, arguing that even though it might reduce the running and total cost, the reactor net power will be reduced with a poor control of the reactivity. Furthermore, it was found that the pump trip transient does not lead to an accident releasing radioactive materials into the environment. Therefore, the elimination of circulation pumps is not related directly to the improvement of reactor safety. Nevertheless, they showed that, under atmospheric pressure, NCBWR experience different forms of instabilities that can happen individually or be superimposed on each other. Further distinction between the forms of flashing was introduced by Furuyaa et al. [8].They divided the flashing instability into two wave forms: intermittent oscillations at high inlet subcoolings and sinusoidal at lower subcooling temperatures.

The intermittent oscillations are characterized by an incubation time before the onset of flashing, while the incubation time is nonexistent in the sinusoidal waves. Furthermore, the period of oscillation is related to the time for single phase liquid to pass through the chimney independent of the heat flux, and inlet subcooling, which suggests that flashing induced instability is a form of density wave instability. Wang et al. [14] clarified that with manipulation of heat flux, at constant pressure, natural circulation system experience four kinds of waveforms namely, intermittent, double peak, sinusoidal, and periodic oscillations. The oscillations frequencies increase in the aforementioned order, with the irregular and period instabilities having the highest amplitude. The intermittent oscillations are characterized by an incubation time for the flashing to build up, they found that the incubation time is inversely proportional to the heating power. At medium and higher heat flux the incubation time vanished and the oscillations become smoother. Yanan et al. [17] showed, by means of the RELAP5/Mod 3.4 code, that at low pressure, the flow can exist as steady single phase or steady two phase with a various degree of instability in between. The degree of oscillations depends on the level of subcooling at the inlet and the interchange between flashing and boiling, which can be intermittent, compound, or sinusoidal oscillations with a decreasing time period.
In this thesis, we will analyze the forms of flashing under forced circulation and how their oscillating characteristics change under the effect of driving forces (frictional and buoyancy). Efforts have been made to understand the effect of geometrical and thermo-hydraulic factors on two phase flow instabilities. Geometrical parameters can be the height of the chimney, the dimensions of the fuel rods, and the flow control valves. As for thermos-hydraulics, it includes the system pressure, the inlet subcooling temperature, and the heating power. At fixed inlet subcooling, it has been discovered that the oscillation duration gets shorter as heating power and/or system pressure increase [7] Increasing the pressure has a stabilizing effect by reducing the unstable flow region and the amplitude of oscillations Manera et el. and Yanan et al. [12] [17]. During the cold start-up procedure, pressurizing the reactor above the critical pressure (750 kPa) eliminates the instability phenomena [17]. Wang et al. (2022) explores the flashing-induced flow instability in the natural circulation test facility which is scaled down from the PWR-type Small Modular Reactor (SMR). The effect of Power and pressure on stability was investigated. At low power, the flow is stable single-phase condition. But with the increase of heating power, relative amplitude of oscillations increases. However, with further increase of power, the amplitude is decreased. On the other hand, the Oscillation amplitudes always decrease with an increase in pressure [15]. Increasing the chimney height have significant stabilization results, while decreasing the inlet flow resistance makes the operation more stable (Yanan et. al [17]). However, Akshay Kumar et al. (2021) [10] proved analytically that flashing induced instability is not affected by the inlet and exit flow restrictions due to the strong coupling between the flow velocity and pressure drop in the system. Overall, Flashing-induced instability causes flow oscillations with a large amplitude which is harmful to the natural circulation system, and the phenomenon needs to be avoided in operating conditions. This thesis will handle the effect of power, system pressure and pump bypass valve on the flashing induced instabilities in a forced circulation system.

1.3. Objectives and Outline

The objective of thesis is to identify the role of the driving forces (frictional vs. buoyance) on the wave characteristics (shape, amplitude and period) during the flash-induced oscillations under force convection. This will be done by handling the following hypotheses, based on literature on NCBWR:

- HYP. 1: Increasing the slope of the external curve dampens the amplitude of the oscillation.
- HYP. 2: Increasing the power applied reduces the incubation time of the wave shape.
- HYP. 3: Increasing the system pressures decreases the amplitude of the oscillations.

2. Methods

2.1. Facility

The experimental facility Fig. 1 is a closed R134a loop consisting of tank, pump, pre-heater, heated section, sight glass, adiabatic riser, and a condenser. The working fluid is driven by a magnetically coupled digital gear pump located below the main tank. The pump is characterized by a maximum speed of 3600 RPM and maximum flow rate 4212 ml/min. A conditioner (heat exchanger) is introduced before the pump in order to assure subcooled single-phase flow into the pump. The heated section inlet temperature is adjusted by passing the fluid through a pre-conditioner after leaving the pump. A bifurcation, before the heater, allows all or part of the flow to bypass the heated section. After the heater, the flow goes through the riser and back to the condenser. The condenser is mounted over the tank, to store the fluid in the tank at saturation conditions. The system pressure is controlled by the saturation temperature of condensation. The condenser is a shell-and-tube heat exchanger, while the pre-conditioner is a fin-plate heat exchanger. The temperatures of the pre-conditioner and

the condenser are controlled by two chillers whose operating temperatures are regulated via interface software. The test section consists of a horizontal heating pipe followed by 5 m vertical U-tube. Inlet restriction (K_i) provides the required pressure drop at the inlet of the heater. The heated stainless-steel section is designed to be electrically heated using the Joule effect, employing a rectified sine wave through 6 electrodes distributed evenly along the pipe. The heating system Fig. 2 is divided into five distinct sections, allowing for independent specification of power to each section. Each section has a length of 400 mm and is characterized by internal and external diameters of 5 mm and 8 mm, respectively. To measure the wall temperature of the heated pipe, several external thermocouples are strategically distributed along the wall surface. Notably, thermocouples located at positions 6 (1117 mm from the inlet) and 10 (1917 mm from the inlet) encompass measurements on the top, bottom, and both sides of the wall, along with an internal thermocouple at the inflow. The two internal thermocouples measure the temperature of the flowing fluid. At the exit of the heated section, and before the adiabatic riser, there is a 1 m long bifurcation. It consists of two parallel arrangements aimed at studying pressure drop characteristics. These arrangements serve different purposes, with one focusing on distributed pressure drop analysis (piping) and the other on local pressure drop analysis (orifice valve). The adiabatic pipe leg is a 1 m long stainless-steel pipe with inner and outer diameters of 5 mm and 8 mm, respectively. Alternatively, the other leg incorporates an orifice valve. This valve offers the flexibility to change the orifice size, enabling the study of various outlet local pressure drops. Throughout this section, the pressure drop is recorded using a differential pressure transducer.Two visualization glass points are present, one at the inlet of the heated pipe to make sure the flow enters as a single phase liquid, and the second is at the outlet to study the two phase flow patterns. Finally, a 5 m high U-tube, installed after the 1 m long adiabatic section, to study the influence of gravity forces on the flow instabilities. The riser Fig. 3 is a 5 mm Quadra capillary hose made of thermoplastic material with polyester reinforcement and thermoplastic cover.

2.2. Instrumentation

The following sensors are employed to acquire the relevant data in the experiment:

- Flow rate: Two Coriolis flow meters are utilized to measure the mass flow rate. These flow meters are positioned immediately after the inlet conditioner and just after the surge tank.
- Absolute pressure: Absolute pressure transducers are strategically placed at various locations, including the condenser, right after the pump, at the inlet and outlet of the heating section, and at the inlet and outlet of the riser.
- Differential pressure: DP cells are employed to measure the differential pressure. For the heated pipe, the differential pressure is measured at multiple points, including the inlet valve, along the heated section, along the 1 m long adiabatic section, and at the outlet restriction.
- Temperature: Temperature measurements are taken at several key points. The flow temperature is directly measured at the condenser, at the inlet of the pump, before and after the inlet conditioner, and at the inlet and outlet of the heated section. Additionally, temperature is measured at two points along the heated section. The exterior wall temperature is recorded at ten points located at the top of the heated section.
- Heating power: The heating power is determined by calculating the root mean square value of the electric current and voltage. Current and voltage values are acquired for each of the five consecutive heated segments along the heated section.

By employing these sensors, comprehensive data is collected on flow rate, absolute pressure, differential pressure, temperature, and heating power, enabling a detailed analysis of the experimental parameters and system performance.

2.3. System calibration

2.3.1 Accuracy of the measurements

Table 1. provides a summary of the accuracy achieved in measuring various relevant parameters. The heat flux measurement involved calibrating the electrical power applied to the pipe against the heat transfer rate to the fluid under steady-state conditions. This calibration was performed for different temperatures and flow rates in the case of single-phase liquid flow, resulting in a final accuracy of 3%. The temperature and heat flux calibrations were part of PhD work of Chiapero [4].

2.3.2 Statistical sampling

Utilizing statistical sampling techniques on a set of measurements can significantly increase the reliability of a reported measurement by minimizing the impact of random errors. These errors arise from various sources

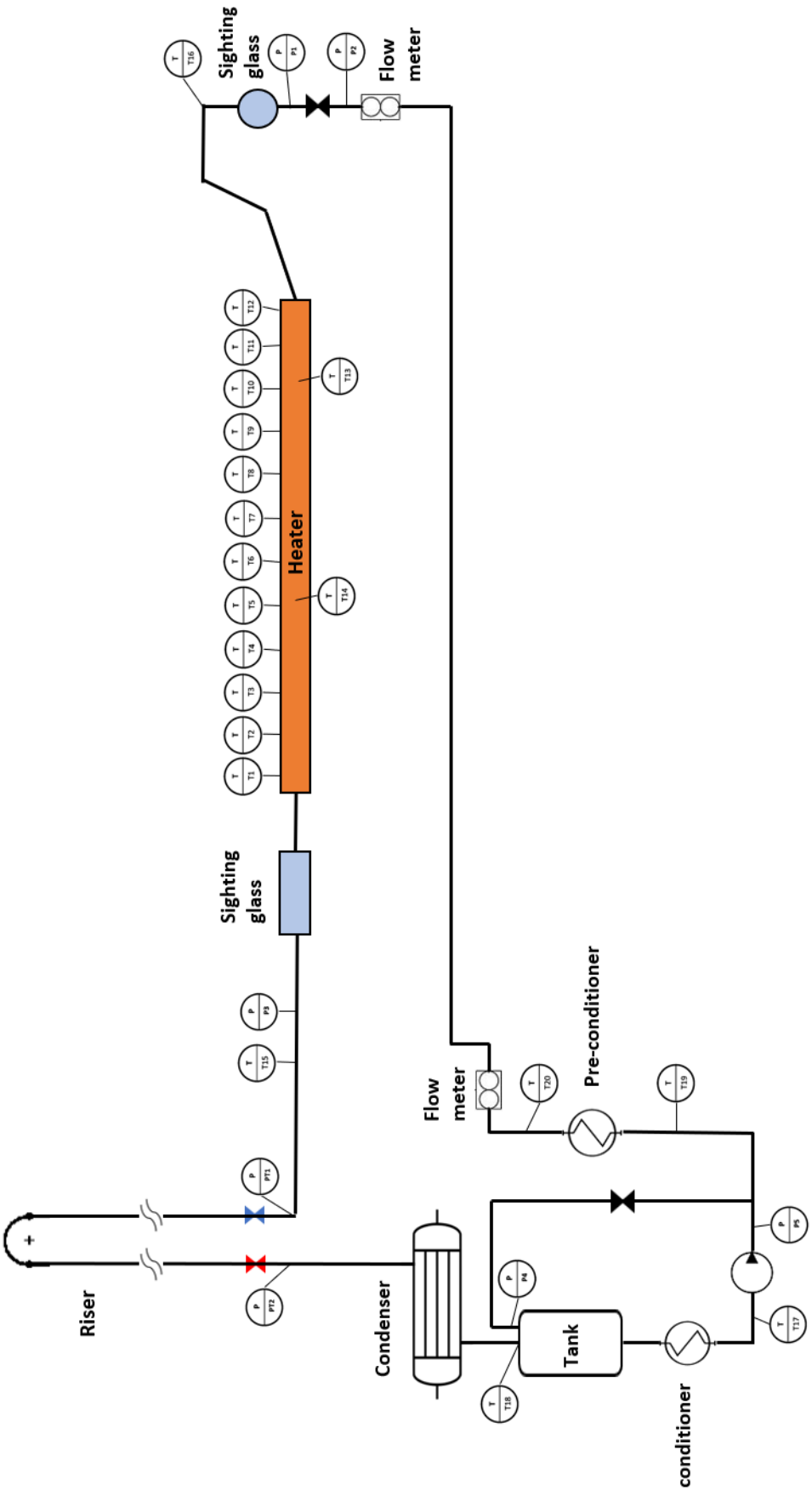

Figure 1: 2D schematic of the test facility

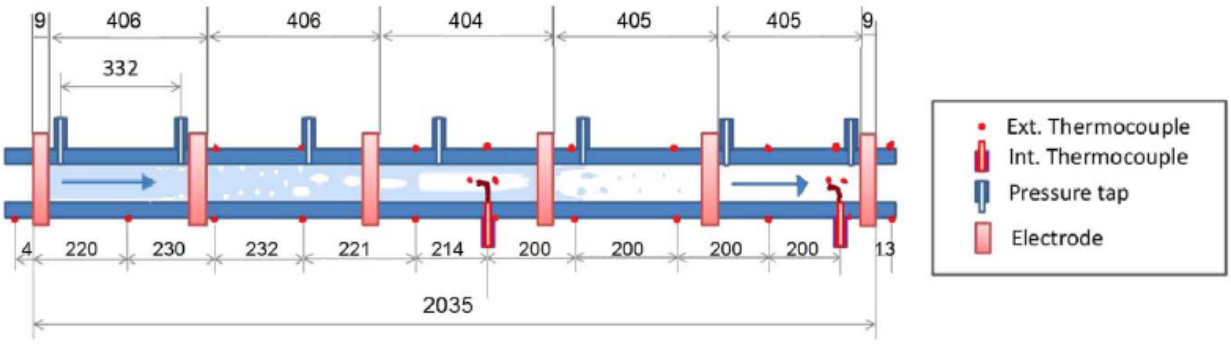

Figure 2: cross section of the heated section with the installed instrumentation

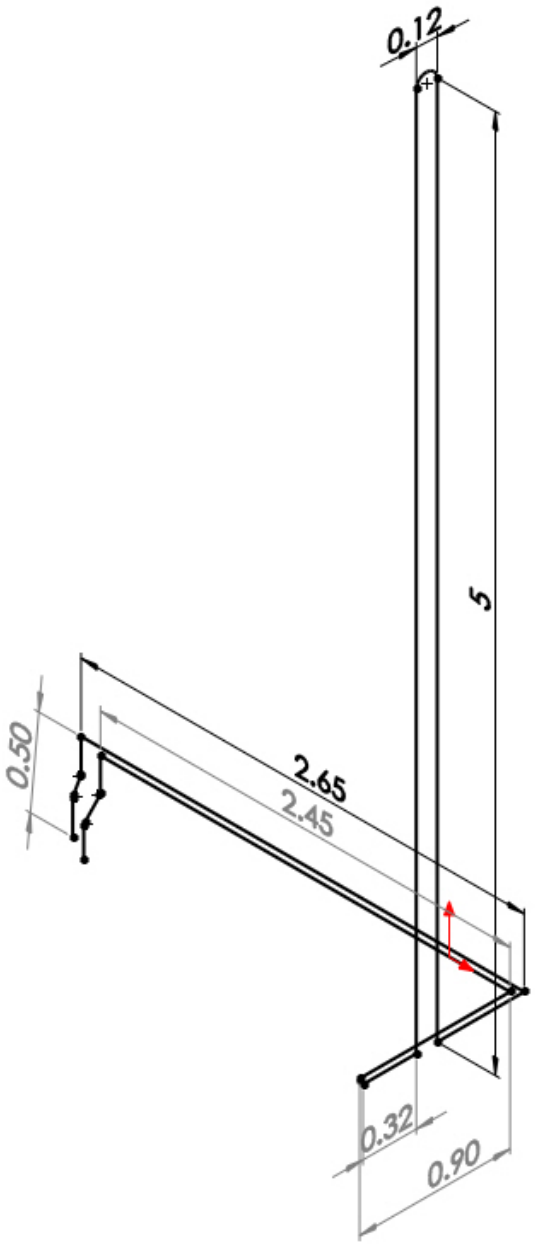

Figure 3: 3D sketch of the riser, dimensions in m

Table 1: Measurements accuracy

Variable	Accuracy	Calibration
Mass flux G	0.2% of the reading	Supplier
Pressure drop ΔP	0.075% full-scale (fs = 50 kPa)	Supplier
Absolute drop P	0.04% full-scale (fs = 25 bar)	Supplier
Temperature T	0.1 K	Chiapero
Heat flux q''	3% of the reading	Chiapero

such as temperature fluctuations, instrumental noise, and inherent fluctuations in the quantity being measured. When conducting experiments, histograms are employed to uncover the characteristics of random errors in the measurements and, in certain cases, to detect systematic errors. Fig. 4 shows the histogram of the mass flux. Each subplot presents a different acquisition time. It can be seen that at higher acquisition time, the distribution of the samples represents a Gaussian distribution. In Table 2, the mean value, the standard deviation, Kurtosis and Skewness are summarized for each sampling time. It can be seen that at 50 s the Kurtosis and Skewness approaches those values of a Gaussian distribution (K=3 and S=0). Based on these observations, the minimum sampling time is 50 s.

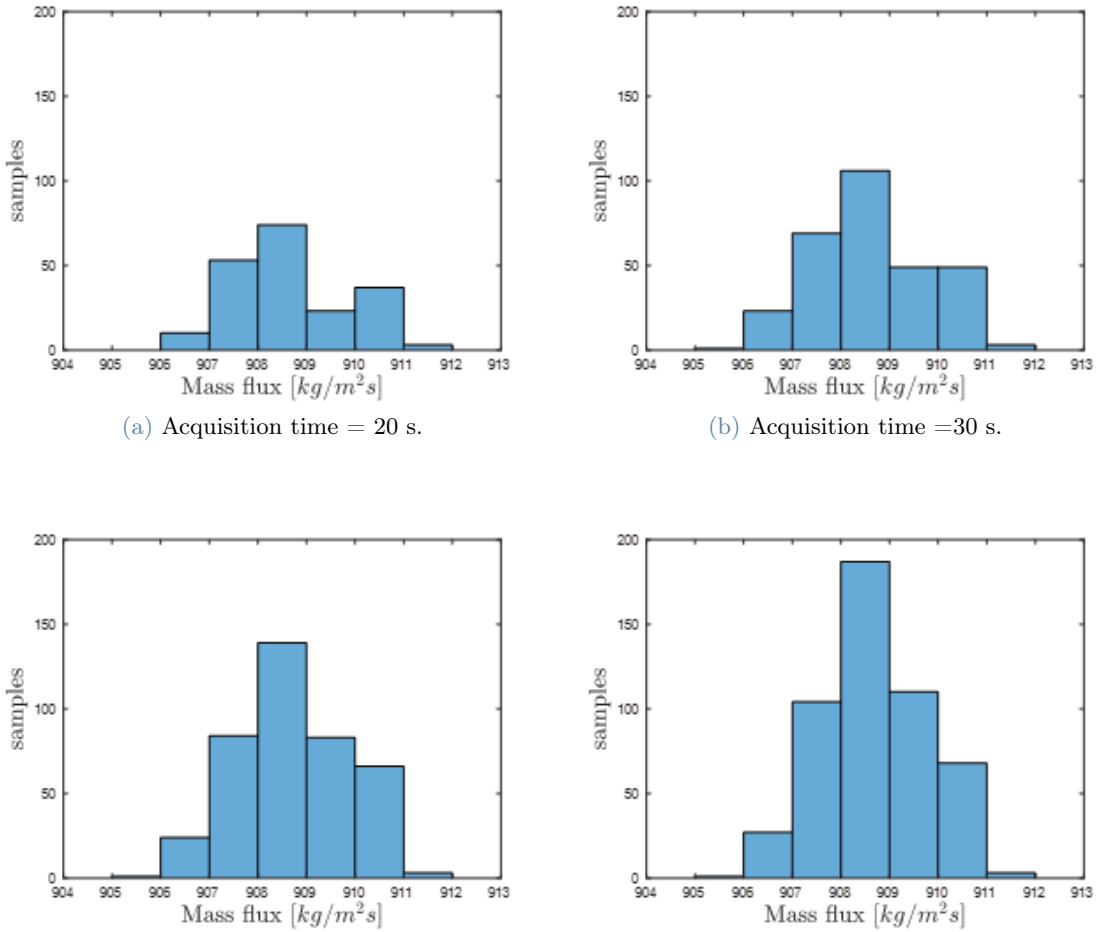

(a) Acquisition time = 20 s.

(b) Acquisition time =30 s.

(c) Acquisition time =40 s.

(d) Acquisition time =50 s.

Figure 4: Histogram of mass flux measurements for different acquisition times

2.3.3 Error propagation

Ruspini [13] ran power calibration for the heating section. Firstly, a digital oscillation scope (LeCroy) was used to obtain the actual shape of the applied voltage and current signals in each of the heated sections. Then, the voltage and current signals obtained with the oscilloscope were integrated numerically to get the DC component of the signal. An integration time corresponding to 20 periods was used to obtain the average values. On the

Table 2: Statistical analysis for the mass flux at different sampling times

Time	Mean	STD	K	S
2 s	908.54	1.28	2.31	0.3652
30 s	908.50	1.29	2.37	0.1443
40 s	908.61	1.24	2.37	0.0392
50 s	908.57	1.18	2.53	0.0593

other hand, the current measure chain used resistance in order to transform the current signal into voltage. Fig. 5 shows the calibrations of current and voltage signals, where The variables $CurrentPC$ and $voltagePC$ are the values measured in the acquisition card. Ruspini, then, estimated the error in the power measurements to be around 3%.

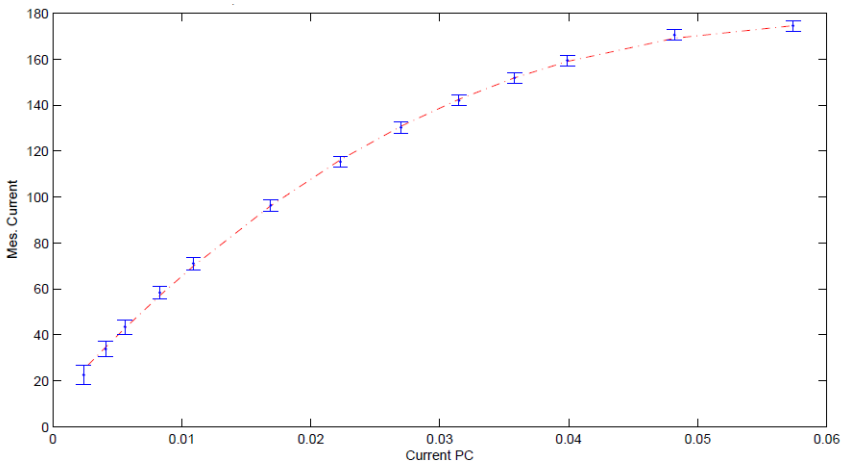

(a) Current signal calibration.

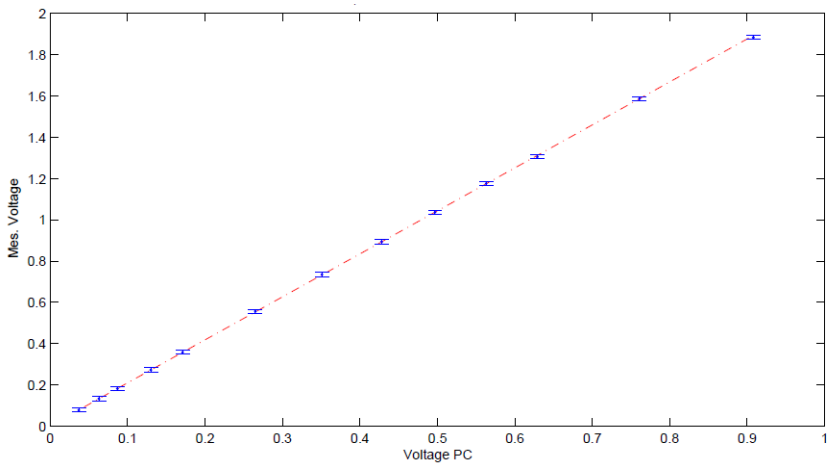

(b) Voltage signal calibration.

Figure 5: Power calibration. the current and voltage signals are calibrated by measuring the integral of the actual current and voltage for each heated section

Similar analysis can be conducted to estimate the error in quality. The vapor quality at the exit of the heated section can be determined by stating a heat balance along the pipe, as follows:

$$x(z) = \frac{\int_{z_0}^{z} q" \pi D_i dz - GA_c cp_l T_{sub}}{GAH_{lv}} \tag{1}$$

Let $x(z)$ represent the mixtrue quality at a specific point $z[m]$ along the heated section. The mass flux rate is denoted as $G[kg/m^2 s]$, the liquid phase specifc heat capacity as $cp_l[J/kgK]$, the enthalpy of vaporization as $H_{lv}[J/kg]$, and the inlet subcooling as $T_{sub}[K]$.

The error propagation formula of a measured quantity can be written as $A = \overline{A} \pm \sigma_A$, where $\overline{A}$ is the mean value of A and σ_A is the error. Applying the averaging rules on equation1 we can calculate $\overline{x}$:

$$\overline{x} = \frac{\overline{q"} A_s - \overline{G} A_c cp_l T_{sub}}{\overline{G} A_c H_{lv}}$$

where A_s is the side area of the heating pipe, and A_c is the cross sectional area of the pipe. The error is calculated as a function of the errors of the variables included in the quality equation. The error of the numerator is given by

$$\sigma_{num} = \sqrt{(\sigma_{q''})^2 + (\sigma_G)^2}$$

then σ_x is calculated as

$$\sigma_x = \overline{x} \sqrt{(\sigma_{num}/\overline{num})^2 + (\sigma_G/\overline{G})^2}$$

Fig. 6 shows the propagation of error for the quality under operating conditions of P=7 kPa, and power=250 W, where the average mass flux is 213.11 kg/m^2s. It can be seen that the value of the error is independent of the inlet subcooling temperature, and quality can be written as

$$x = \overline{x} \pm 0.32$$

The error is of the same order as the mean value, which is due to the simplifications used in the calculation of the quality of a two phase flow.

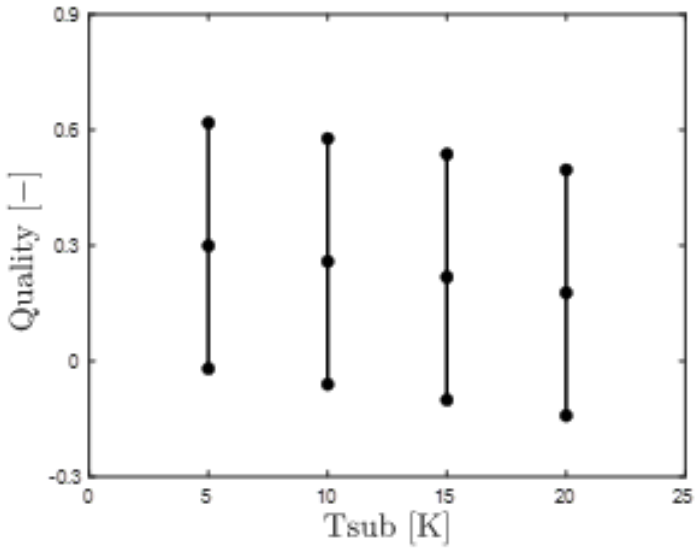

Figure 6: Error propagation of the vapor quality at the exit of the heater at P=7 kPa, and power=250 W

2.4. Experimental Procedure

The operational conditions are determined by four key parameters: the inlet absolute pressure (P_{in}), the inlet subcooling ($\Delta T_{sub,in}$), the heat flux (q"), and the pump bypass valve. These parameters are controlled by specific components: the pressurizing tank regulates Pin, the condenser controls ($\Delta T_{sub,in}$), the main heater manages the heat flux, and the globe valve adjusts the pump bypass. In situations where instability is present, the inlet pressure exhibits periodic oscillations with small amplitudes compared to its average value. Conversely, fluctuations in the inlet subcooling are minimal and comparable to the uncertainties of the instruments used for measurement. Therefore, the time-averaged values of the inlet absolute pressure and inlet subcooling serve as nominal references for the conditions.

During the experimental tests, the total pressure drop, absolute pressure, mass flow rate and wall temperatures were directly measured with the above mentioned transducers, while the heat transfer coefficient and the fluid quality were calculated from the mass flow rate, temperatures and heat fluxes recorded. The measurements were registered by a computer equipped with a National Instruments NI RIO data acquisition system. The temperatures, absolute pressure, pressure differences and mass flow rates were acquired at a frequency of 2 Hz. For every experimental data point reported, 120 data points were measured during a minute, and treated statistically. The chiller setting temperatures, pump speed, and electric heaters power are controlled through

LabVIEW software. The collected data were subjected to statistical analysis for further evaluation and interpretation. For the temperature measurement, type-T thermocouples with 0.5 mm diameter were used. The absolute pressure at the inlet and outlet of the heated section was also recorded and was used for checking the saturation temperature T_{sat} of the fluid based on the equilibrium thermodynamic properties calculated with REFPROP.
The pump curve Fig. 7 was obtained by running the rig in steady state single phase liquid operation. The bypass valve was 1/2 turn open and the inlet restriction valve to the heater was gradually opened from almost zero to fully opened. The readings were recorded for at least 50 s for each open of the inlet valve. The same readings were repeated three times and the average values of mass flux and pressure drop were used to plot the pump curve. A polynomial function was fitted to the recorded values and the plot range was extended as shown.

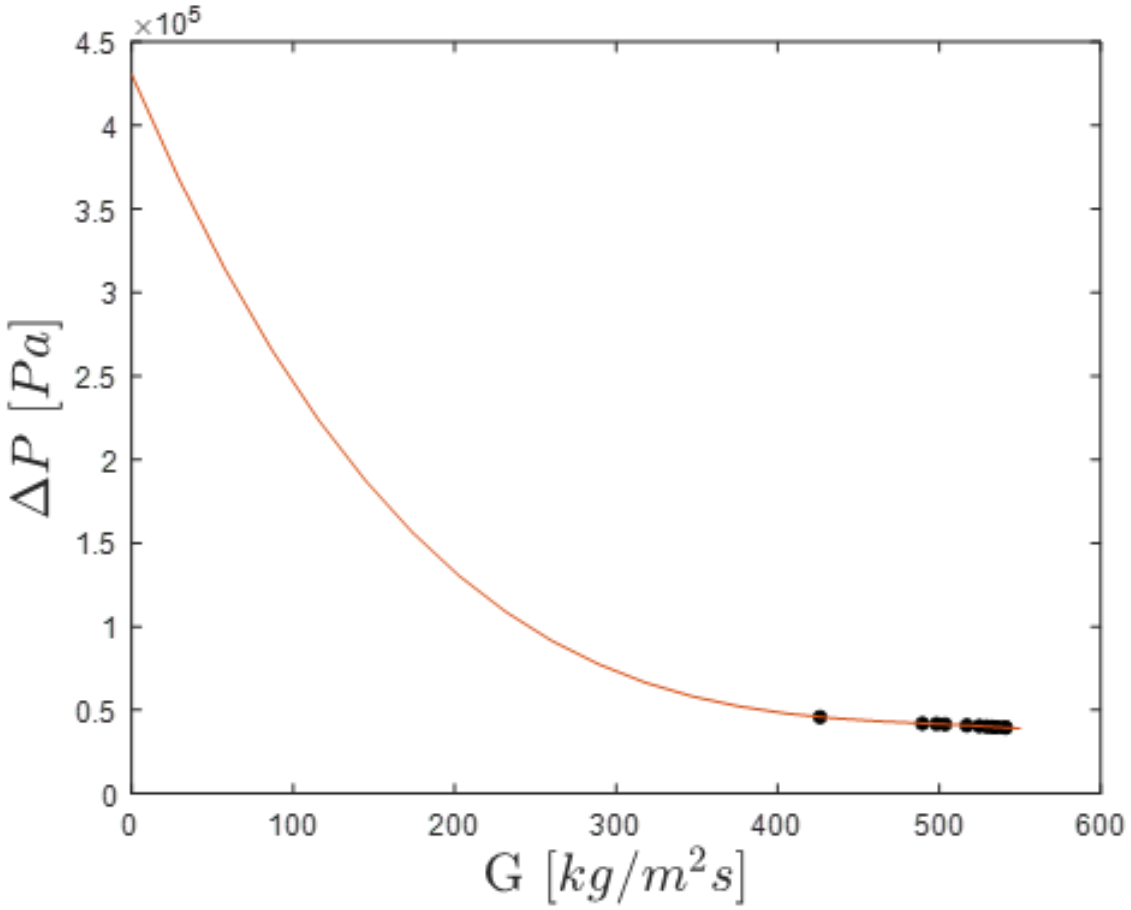

Figure 7: Pump characteristic curve for 1/2 *turn bypass valve*

The instantaneous readings were monitored via MATLAB. The aforementioned operating parameters were set to the desired study case and the system runs until steady state was reached. The parameters were adjusted so that the monitored ΔT_{sub} at the heated section exit was close to saturation. This case can be reached by either reducing the mass flux at a constant heating power or increasing the heat flux at a constant flow rate. After stabilization, we tried to trigger the flashing instability by applying a sudden change in one of the parameters (G, q_J) while keeping the remaining factors constant. This procedure led to one of three scenarios: stable case, damped and unstable case as shown in Fig. 8. A case is stable if it moves to a new stable point, whether there were oscillations or not. While unstable case, the system is subject to self-sustained oscillations.

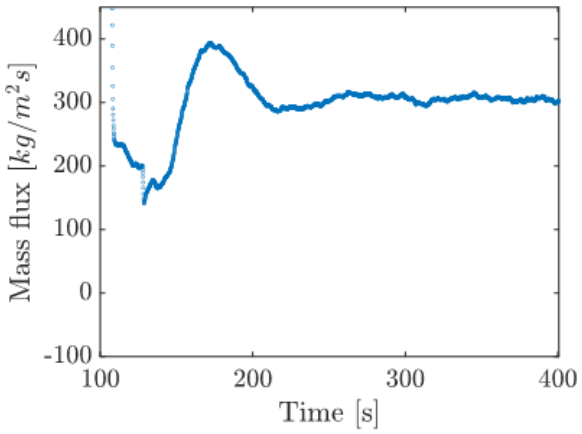

(a) Stable point.

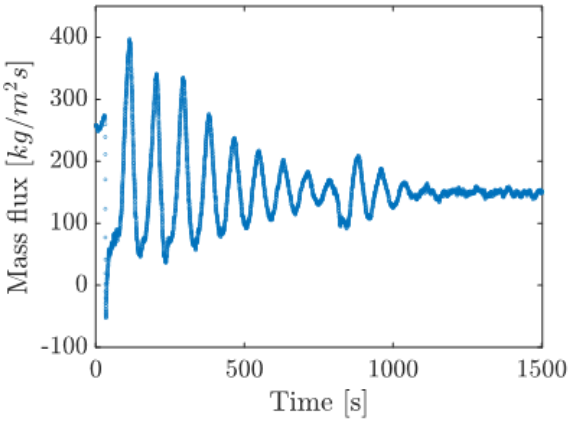

(b) Damped oscillations.

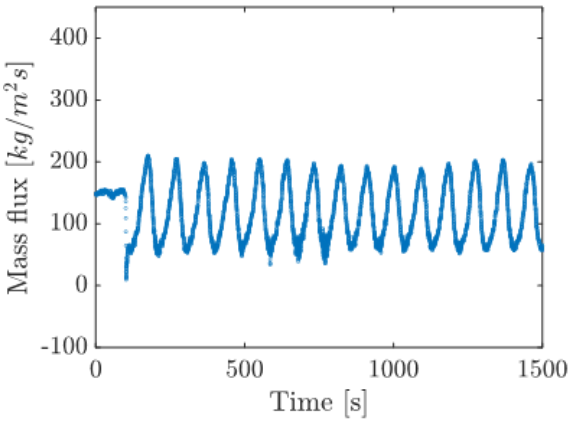

(c) Stability.

Figure 8: ***Stability threshold***

3. Results

The objective of this experimental study is to examine the occurrence of flow instability and its correlation with various parameters in the forced circulation test facility. Following the procedures outlined above, the experiments were conducted. In this section the data obtained from the acquisition system are presented.

3.1. Instability Test

Fig. 9a shows the system transient state. By gradual increase of the heating power, The system became unstable with an increasing amplitude of oscillations. The oscillations were triggered at power $340W$, and remained till the end of acquisition Fig. 9b , while the system pressure was $7.63bar$. Eventually, the amplitude stabilized and an unsteady state with self sustained oscillations was acquired Fig. 10. The system pressure at the unsteady state is depicted in Fig. 10b.

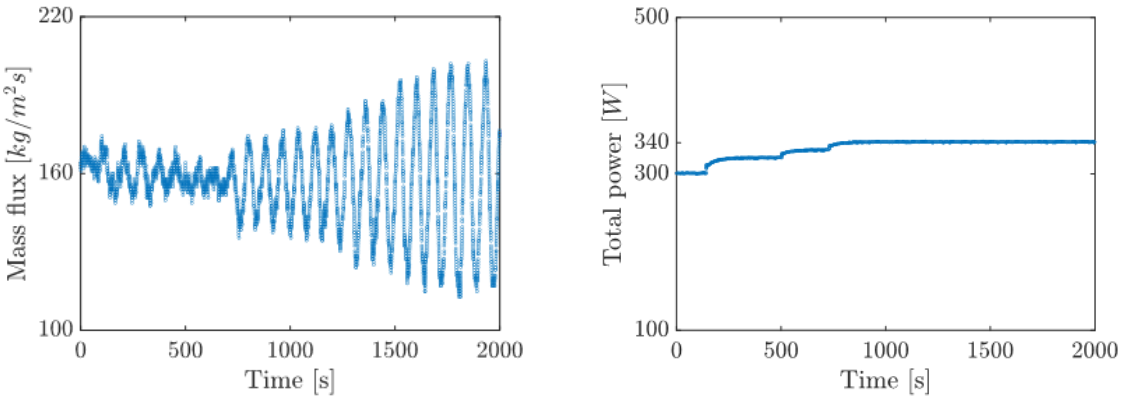

(a) Mass flux curve.

(b) Power curve.

Figure 9: Transient state

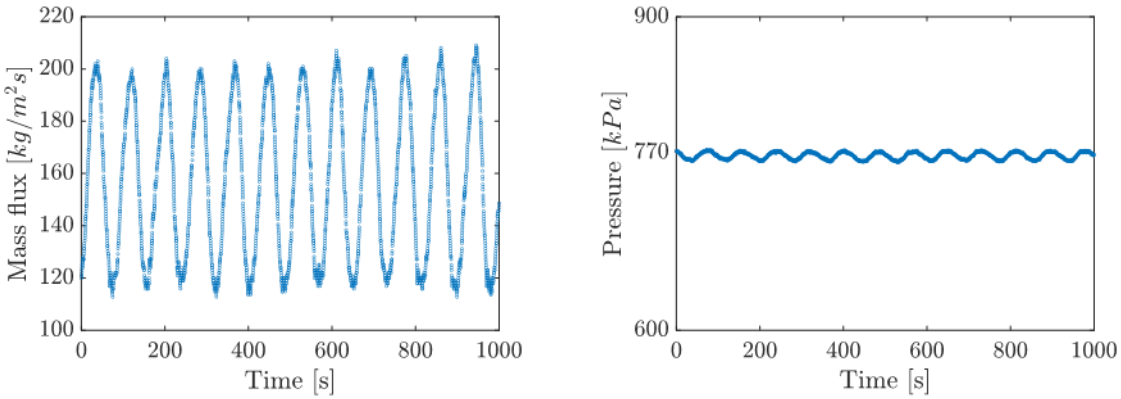

(a) Mass flux curve.

(b) Pressure curve.

Figure 10: Unsteady

3.2. Oscillation types

At high heat flux and 7.5bar pressure, the oscillations were triggered by sudden drop in the mass flux, then the heating power was reduced in 50W steps at a time. At low heating power ($100 - 200W$) the shape of the oscillation is irregular but periodic Fig. 11. At medium power ($250W$) the shape of oscillations is pure sinusoidal with zero incubation time, as shown in Fig. 12. Finally, at high heat ($300 - 450W$) the incubation time is increased and the wave takes an intermittent shape Fig. 13. In subplots b of each case the quality of the flow at the exit of the heating section is calculated according to Eqn. 1, while the local saturation temperature T_{sub} and the temperature at the exit ($T13$) are plotted in subplots C.

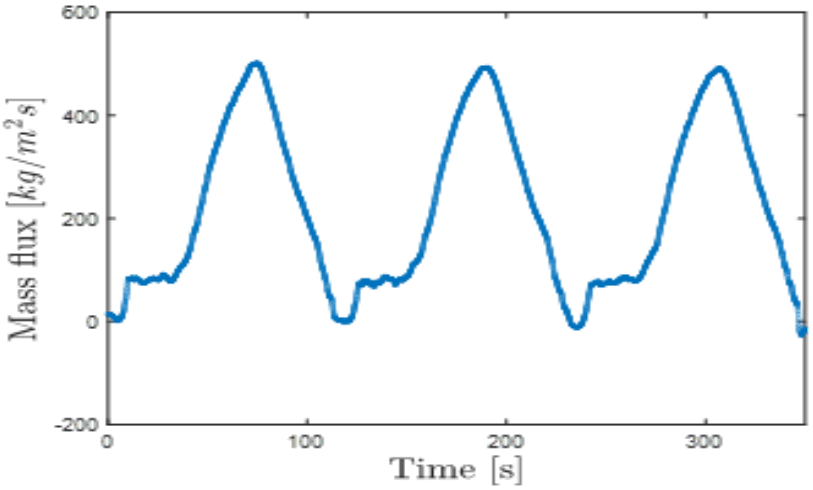

(a) Mass flux curve.

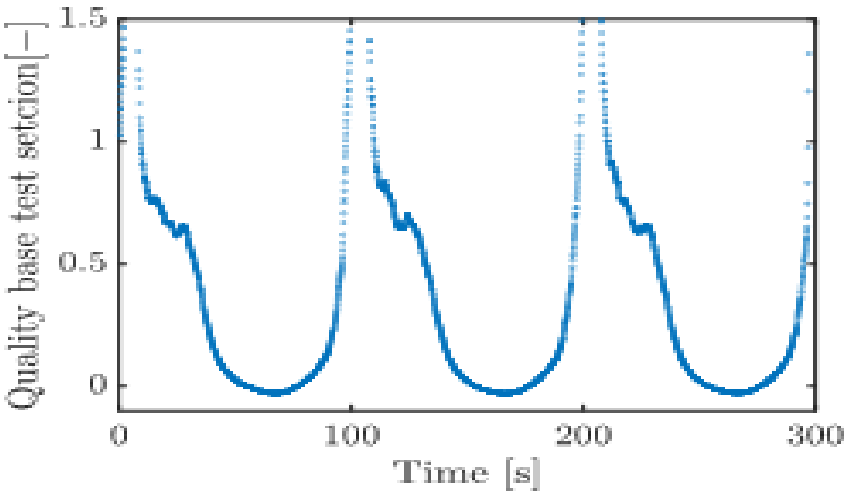

(b) Void fraction at the heater exit.

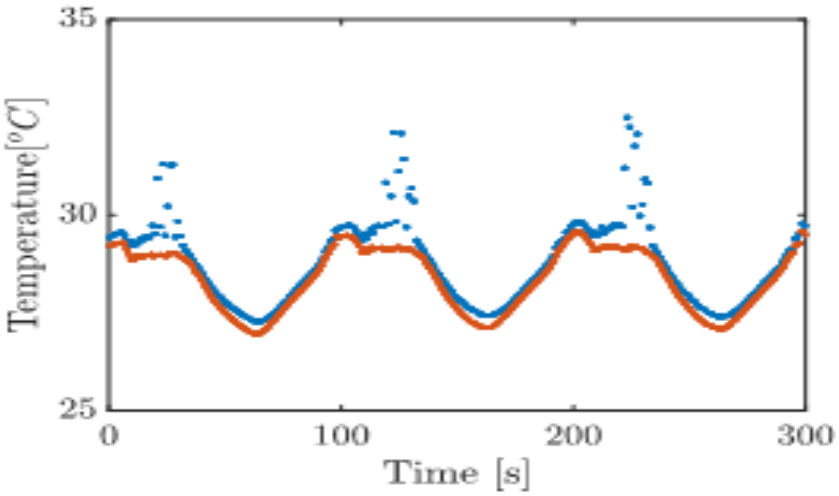

(c) Temperature at the heater exit.

Figure 11: Irregular intermittent regime

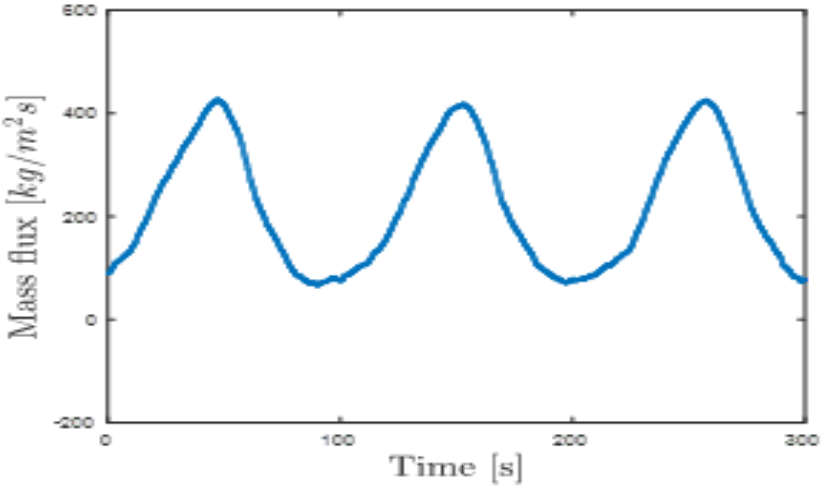

(a) Mass flux curve.

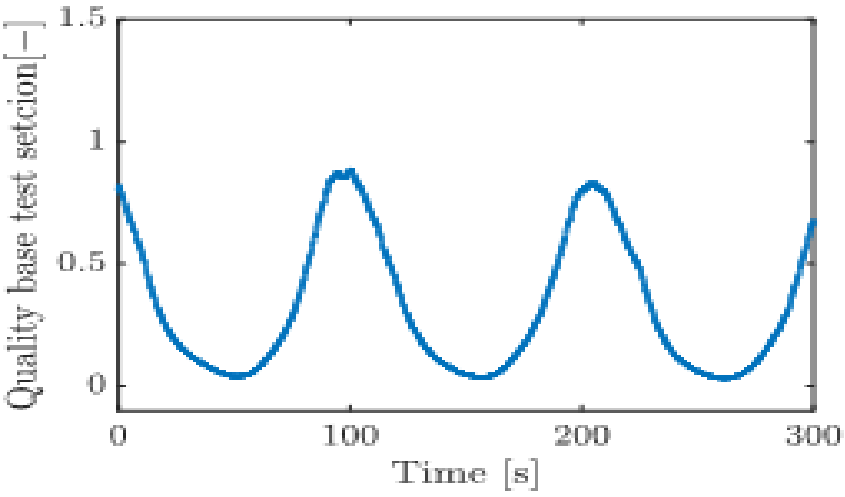

(b) Void fraction at the heater exit.

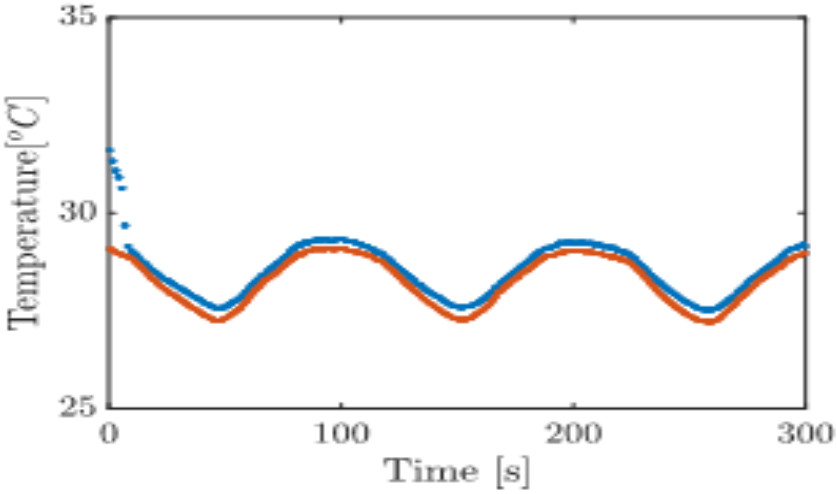

(c) Temperature at the heater exit.

Figure 12: Pure sinusoidal regime

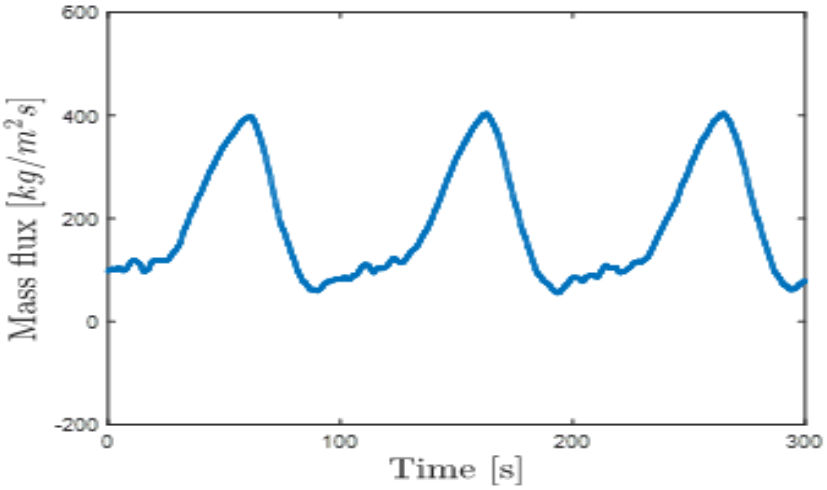

(a) Mass flux curve.

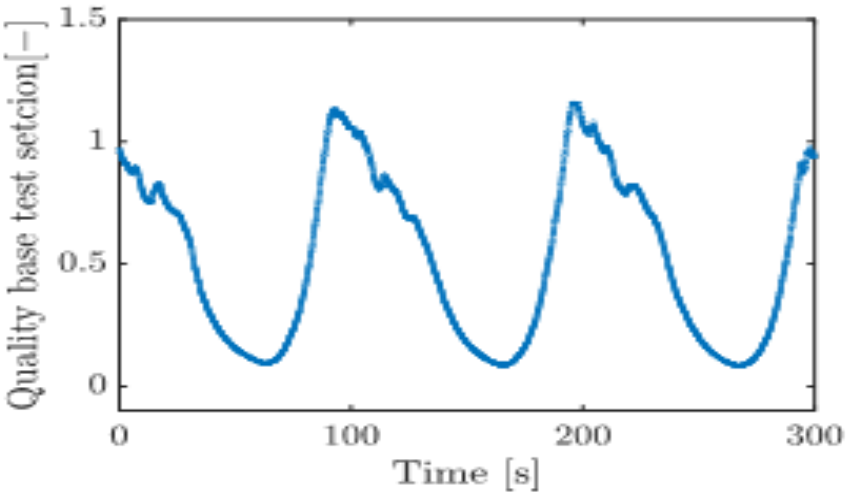

(b) Void fraction at the heater exit.

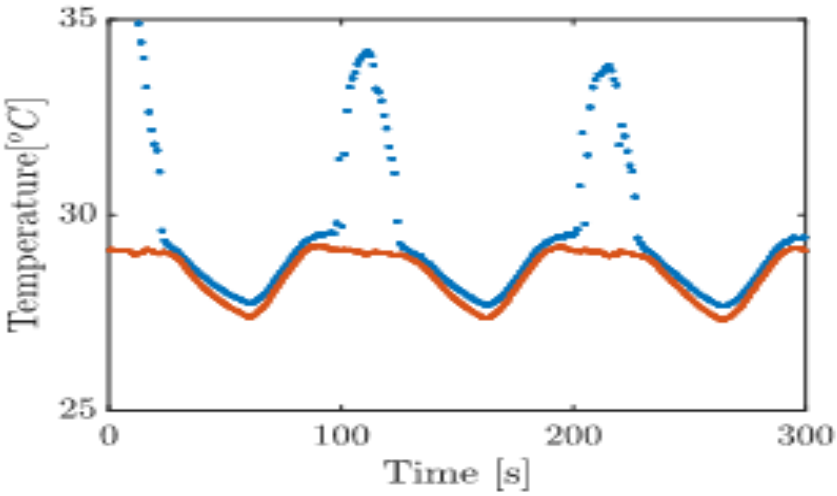

(c) Temperature at the heater exit.

Figure 13: Intermittent regime

3.3. Hyp.1

Fig. 14 shows the effect of closing the pump bypass valve on the amplitude of oscillations. Under the same operating conditions, the instability was triggered and the mass flux oscillations were captured. Figures 14a, 14c, and 14e show the velocity oscillations. The pressure limit cycle is for the three cases is shown in figures 14b, 14d , and 14f. The pressure represents the change of the pressure difference between $P4$ and $PT2$, Fig. 1, against the mass flux. The slope of each pressure limit cycle was obtained by curve fitting the data points.

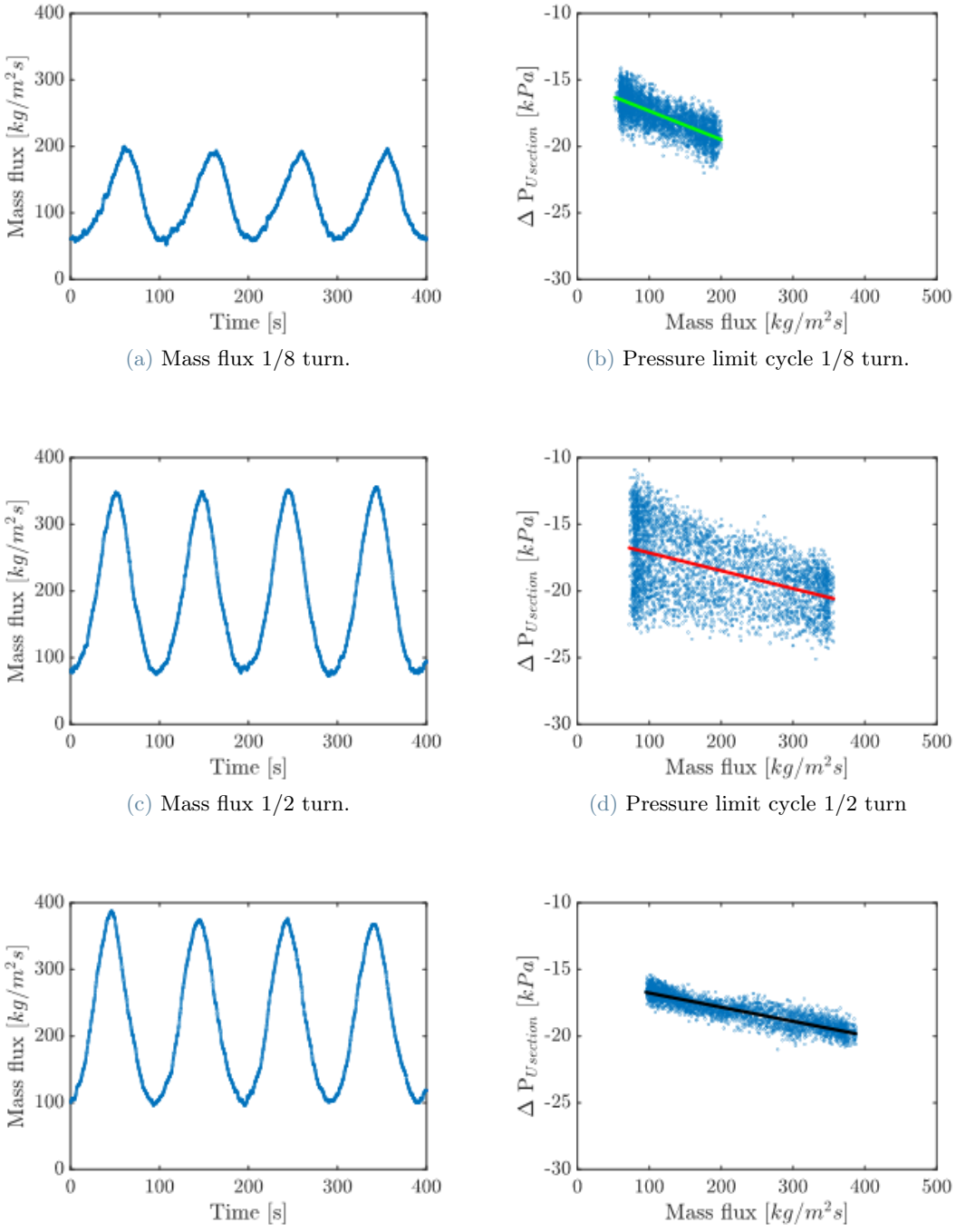

(a) Mass flux 1/8 turn.

(b) Pressure limit cycle 1/8 turn.

(c) Mass flux 1/2 turn.

(d) Pressure limit cycle 1/2 turn

(e) Mass flux 1 turn.

(f) Pressure limit cycle 1 turn

Figure 14: Pump bypass valve effect on the oscillations

The slopes are overlapped in Fig. 15. Green line is 1/8 turn slope, red line is 1/2 turn and black line is the slope of 1 turn opened bypass valve. The plot shows how the pump curve slope is flatter with higher open of the bypass valve.

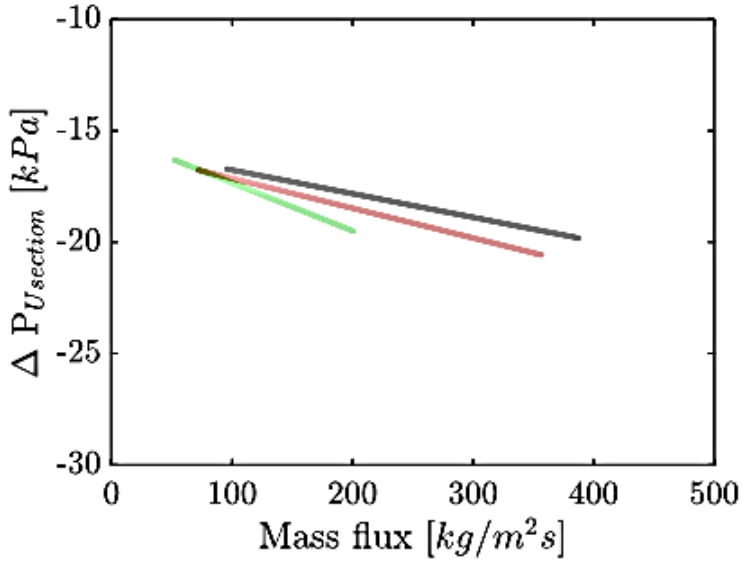

Figure 15: Superimposed slopes of the 3 bypass valve positions

3.4. Hyp.2

Fig. 16 shows the effect of power on the instability's amplitude and frequency. The power was reduced in sudden steps from 400 W to 50 W Fig. 17a. The system was left to oscillate about 5 cycles before the power was changed. In Fig. 17b the temperature at the exit of the heating section, $T13$ Fig. 1, is plotted against the saturation temperature.
The amplitude of oscillation is plotted against the corresponding heating power as shown in Fig. 18a. The amplitude is calculated as $G_{max} - G_{min}$. The period corresponding to each Power is calculated as the time difference of two successive maximum values of mass flux $t_{G_{max1}} - t_{G_{max2}}$.
Fig. 19 shows how the wave shape changes with increase in power. For each heating power, ranging from 100 W to 400 W, The system as left to oscillate about 5 cycles before the power was changed to make sure the oscillations were sustained.

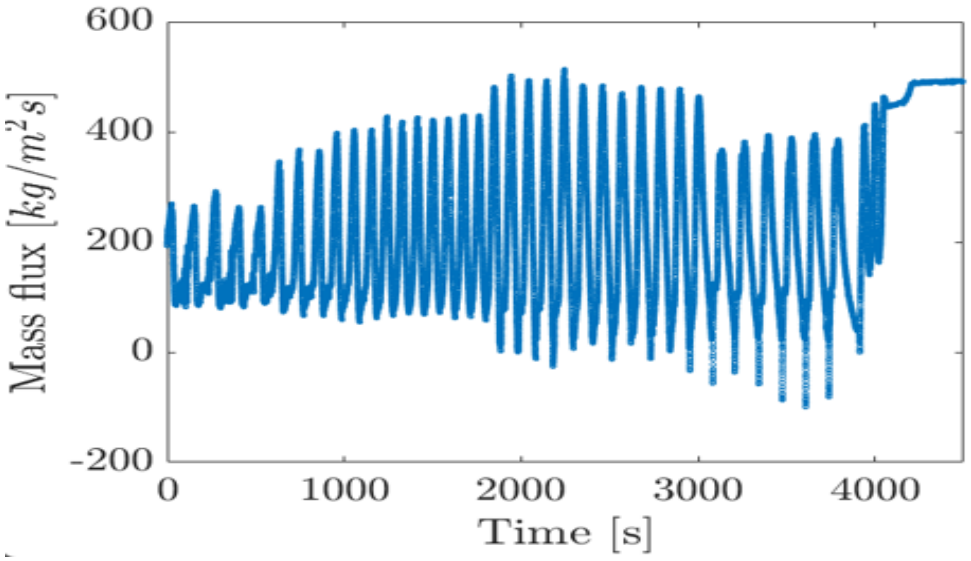

Figure 16: Mass flux oscillations.

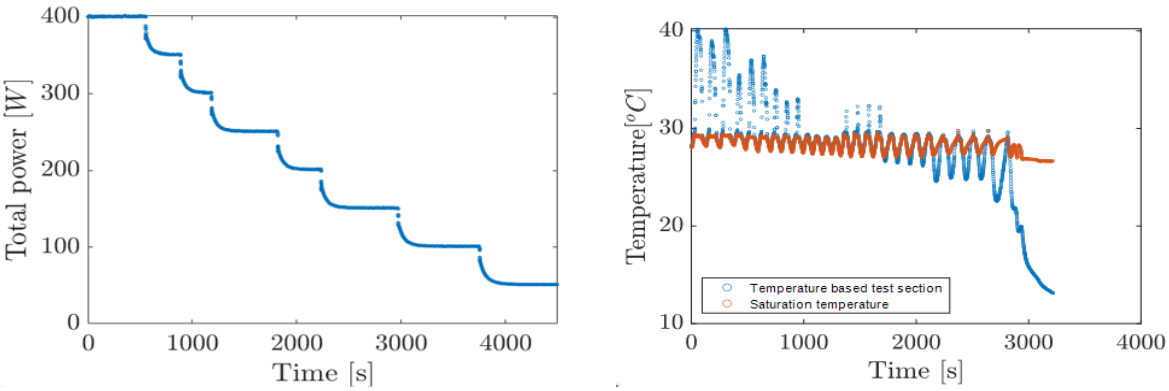

(a) Power curve. (b) Temperature at the exit of the heater.

Figure 17: Heating power effect on the oscillations

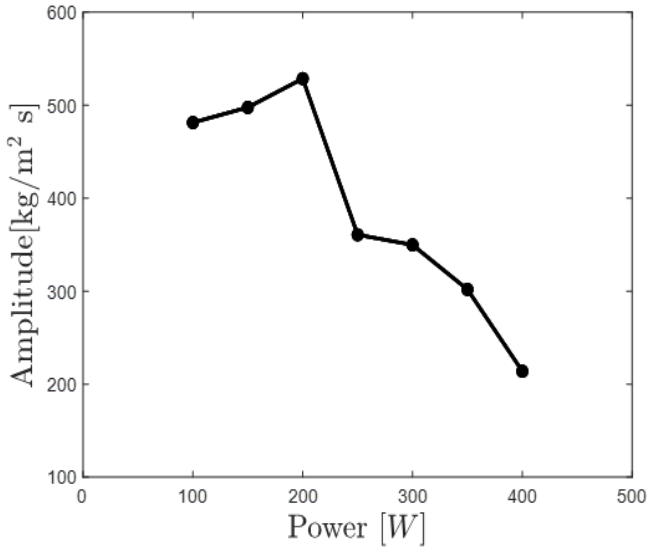

(a) Amplitude.

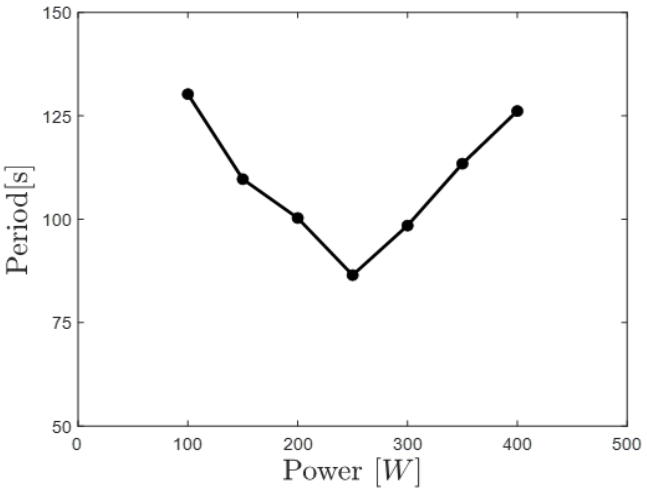

(b) Time period.

Figure 18: Heating power effect on the wave characteristics

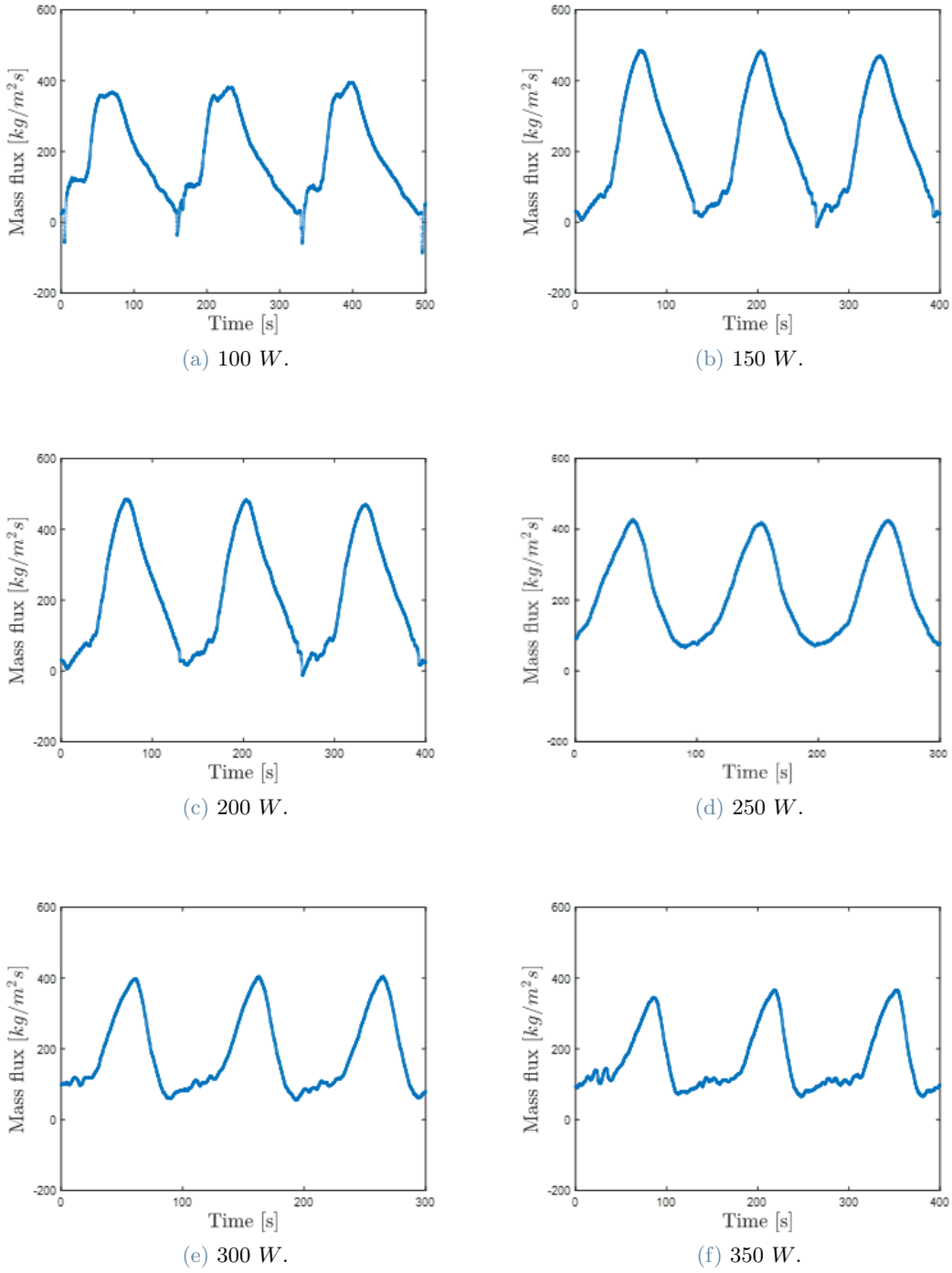

(a) 100 W. (b) 150 W.

(c) 200 W. (d) 250 W.

(e) 300 W. (f) 350 W.

Figure 19: Heating power effect on the wave shape

3.5. Hyp.3

AT a power of 300 W the oscillations were triggered by sudden change in flow rate and the system pressure was increased gradually by controlling the saturation temperature of the tank $T14$ Fig. 1. The system was running for at least 500 seconds under stable condition before the value of pressure the was increased Fig. 20b. The mass flux oscillations due to the increasing pressure are shown in Fig. 20a.

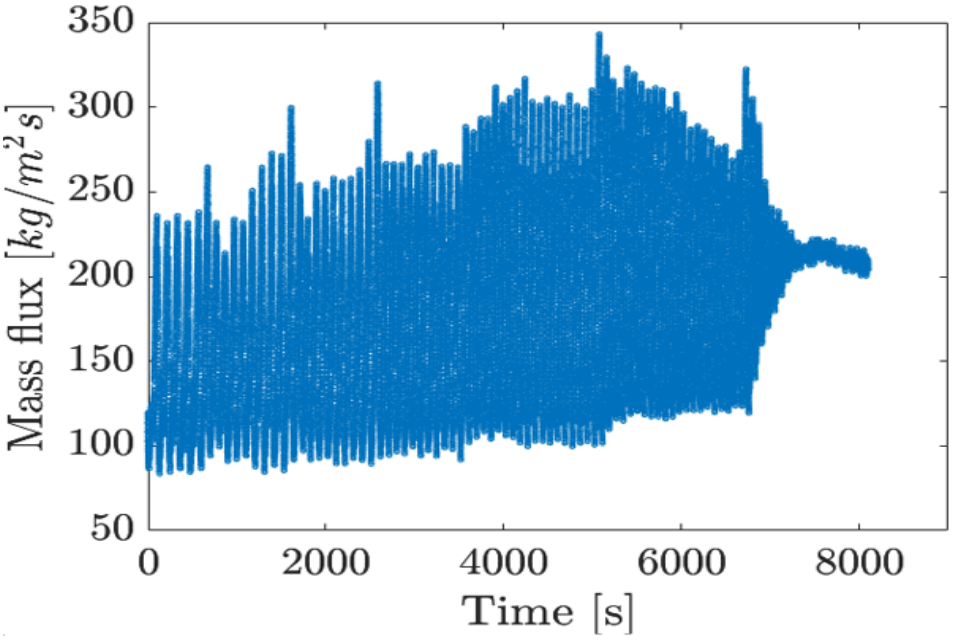

(a) Mass flux oscillations.

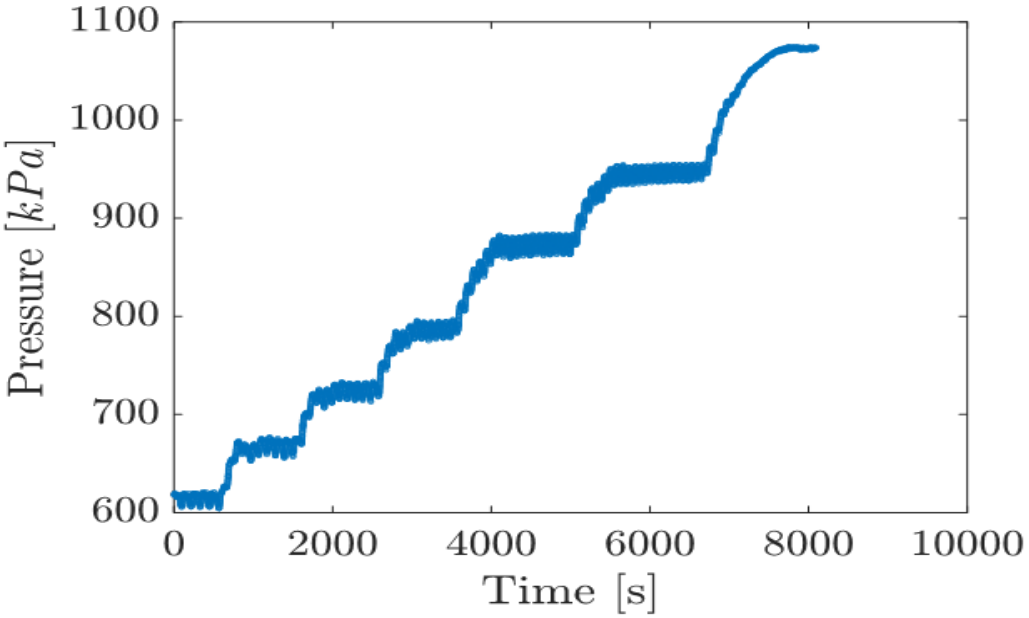

(b) Power curve.

Figure 20: System pressure effect on the oscillations

The effect of system pressure on the amplitude is presented in Fig. 21a while the impact on the oscillation time period is shown in Fig. 21b. The amplitude corresponding to each pressure is calculated as $G_{max} - G_{min}$ and the period is the time difference $t_{G_{max1}} - t_{G_{max2}}$.

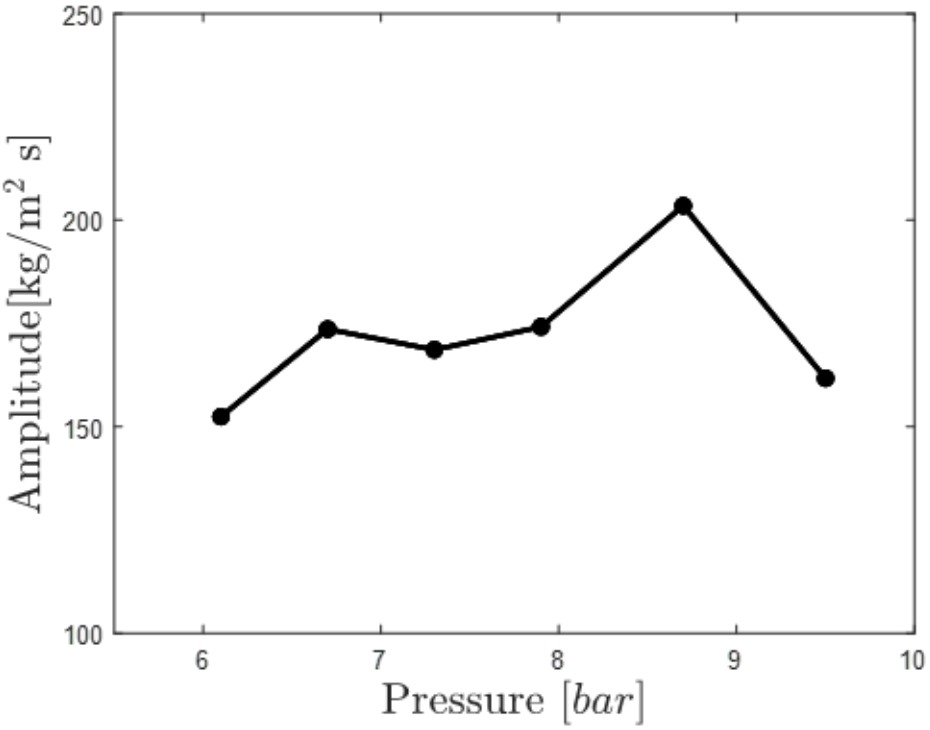

(a) Amplitude.

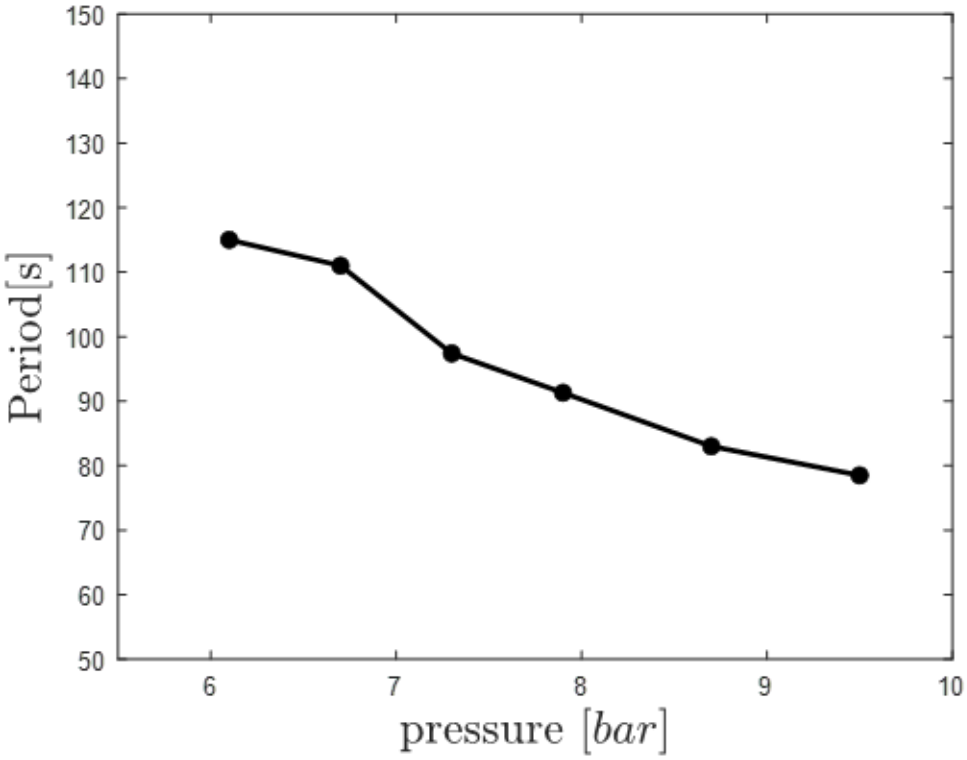

(b) Time period.

Figure 21: System pressure effect on the wave characteristics

4. Discussion

4.1. Instability test

By a gradual increase in the heat flux, 10 W steps, thermohydraulic instabilities were observed. The flow rate was oscillating with high amplitude and frequency. The pressure and temperature were oscillating with small amplitude, thus they were considered constant around the average value of oscillation. The thermal states of the system are as follows:

- Steady state:
  It is single phase liquid state with stable flow rate, temperature and pressure. Before triggering the instability, the system must run in a stable steady state for at least 60 seconds. Steady state experiments were carried out to derive the pump curve as well as having data available for single phase validation.
- Transient state Fig. 9:
  At 340 W, the system started to oscillate with a diverging amplitude. The increased vapor quality at the heater exit led to higher density difference which increased the buoyancy force. The driving force term will be called on the buoyancy force and it is expressed as follows,

$$F_d = \Delta\rho g H \tag{2}$$

  where F_d, $\Delta\rho$, g, ΔH, are the driving force, density difference between the two phases of the flow, gravity, and the height of the riser. When the flow oscillates, the equilibrium between the driving and resistance forces of forced circulation is disrupted. The flashing instability is triggered when the buoyancy force overcomes the frictional force in the system.
- Unsteady state Fig. 10:
  The amplitude stabilized and the wave took a pure sinusoidal shape with high frequency. While the mass flux was oscillating with high amplitude, the system pressure was slightly oscillating around 770 kPa which why the average value of pressure is taken considered to be constant through oscillation. The pressure oscillates due to the vapor propagation in the riser. The occurrence of flashing causes a rapid increase in fluid velocity, followed by the subsequent condensation of vapor through the down-comer. This sudden acceleration can trigger a feedback loop within the forced circulation system, resulting in the formation of flow oscillations with a specific periodicity. Flashing significantly impacts the mass flow rate, particularly at low pressures where the hydro-static head is highly sensitive to it. Consequently, the presence of a phase mismatch between flow, void fraction, and driving head leads to the emergence of self-sustained oscillatory patterns.

4.2. Oscillation types

1. Irregular intermittent oscillations Fig. 11:
   At low heat flux, the oscillations took an irregular repetitive shape. It is characterized by high amplitude and long time period. The cycle starts with close to zero flow rate which causes complete evaporation at the heater exit. As shown in Fig. 11b, the void fraction is much higher than 1 (super-heated vapor). As the Quality increases, the void propagation increases the flow gradually, But condensation takes place in the horizontal piping connecting the heater to the adiabatic riser. As a consequence, the quality drops sharply until the flow becomes two-phase. During this time the mass flux is almost constant and this is called the incubation time. As the quality drops even further, the flow enters the riser as subcooled liquid and the flow temperature at some point is equal to the local saturation temperature and flashing is induced. The vapor bubbles grow due to drop in hydrostatic head, which pushes more flow outside the riser and causing sharp increase in the flow rate. Due to the increased flow rate, the heated section inlet temperature drops as seen in Fig. 11c. By the time the mass flux reaches as maximum, the quality is minimum, which increases the subcooled liquid reserve in the riser, which -in turn- condenses the front wave of the propagating flashing and the flow rate starts dropping sharply. The inlet subcooling drops again because of the reduced mass flow rate and boiling is initiated, shown in Fig. 11c and Fig. 11b the temperature and quality start increasing until they reach maximum values which induces the next cycle of oscillation.
2. Pure sinusoidal oscillations Fig. 12:
   Under medium heat flux, the oscillation is sinusoidal and the incubation time is vanished. The instability is induced by boiling in the heater and enhanced by flashing in the riser. The perfect synchronization between the temperatures in Fig. 12c characterizes this type of flashing. The flow leaves the heater always as two phase flow as seen in Fig. 12b, which means that continuous boiling is the main trigger of the oscillations. The flow is then condensed in the piping to the riser and flashing is induced, which gives the high jump in amplitude.
3. Intermittent Oscillations Fig. 13:

With further increase in the power, The incubation time increases and with it increases the time period of oscillations. At low flow rate, $T13$ increases above the corresponding saturation temperature Fig. 13c and the vapor quality becomes slightly higher than 1 (Fig. 13b). The temperature cools down in the adiabatic test section, and other components such as the condenser and horizontal piping, which causes a slight increase in the flow rate with small fluctuations due to eruptions from condensed bubbles (geysering). By the time the temperature approaches saturation and the quality gets close to zero, the flow enters the riser as subcooled liquid and the flashing is induced at some point in the riser which increases the flow to max Fig. 13a. Due to the high flow rate, the inlet temperature is reduced and the quality increases towards a maximum and the cycle is repeated.

The waves shape of forced circulation are similar to the ones mentioned in the work of Wang [14] for a natural circulation system. Based on the discussed types of flashing, the incubation time is affected by the structure of the riser i.e., longer horizontal piping and higher riser extends the incubation time when the flow leaves the heater with a quality close to or higher than 1. The geometry of the riser controls the size of subcooled liquid storage which suppresses the propagating wave of flashing. The instability is a combination of boiling, geysering and flashing, where flashing is more dominant at medium to lower heat fluxes.

4.3. Hyp.1

The bypass valve controls the slope of the pump curve. The more the valve is opened, the flatter is the slope Fig. 15. The effect of the valve open on the oscillation amplitude is obvious when the mass flux for 1/8 and 1/2 turns are compared, figures 14a and 14c respectively. The amplitude is almost doubled but the period does not seem to be affected. The effect of the pump slope is strongly attenuated between 1/2 and 1 valve turns. As seen in figures 14c and 14e the increase in amplitude is about 15%. The increase in amplitude can be reasoned by the slopes as shown in Fig. 15: for the same change pressure drop $\Delta P_{Usection}$ the change of the flow rate will differ based on the corresponding slope i.e., the green line (1/8) turn will give a smaller change in the flow rate compared to the black line (1 turn).

4.4. Hyp.2

The heating power plays a big role in determining the shape, amplitude, and frequency of oscillations. From Fig. 17 the oscillations change with each step reduction in the power until the power is too small to evaporate the flow and single phase liquid is retained at $50W$, Fig. 16. Fig. 17b shows the phase shift between $T13$ and T_{sub} as the power changes, it becomes clear that the shape of oscillation is sinusoidal only when the temperatures are synchronized otherwise the oscillations take an irregular shape and the incubation time increases. Fig. 19 gives a closer look on the distinct wave shapes evolved by changing the power. For power less than 250 W the waves take an irregular intermittent shape, for 250 W pure sinusoidal and for higher than 250 W it is intermittent. At 400 W the flashing is suppressed and the big peak amplitude is comparable with the amplitude of the fluctuations caused by geysering. The effect of power on amplitude is clarified in Fig. 18a where the amplitude keeps decreasing with the increase of power, which means that the increase of power suppresses the flashing and causes the reduction in the high amplitudes, similar to the results of natural circulation given by Wang [15]. This shows that flashing is more dominant and dangerous at low heat fluxes. As for the time period, Fig. 18b shows that the lowest period is for the pure sinusoidal oscillations at 250 W and the other two types of flashing have similar frequencies. This can be reasoned by the zero incubation time of sinusoidal oscillations, since the incubation time is the main reason behind the long periods for the other waves.

4.5. Hyp.3

Starting from system pressure about 6 kPa, the effect of the pressure on the flashing oscillations is observed. from Fig. 20a the oscillations are present, with a comparable amplitude, until the pressure is too high which suppresses the instabilities around 10 kPa and the single phase steady flow is restored. Increasing the pressure means increasing the friction force which put resistance against the driving force. It results in a decrease in the density difference between the vapor phase and the liquid phase, as well as a decrease in the latent heat of vaporization. As a consequence, the fluid becomes more prone to vaporization, making it more challenging for the system to generate sufficient driving force under high-pressure conditions. As a result, the self-sustained oscillation is weakened or completely eliminated, and once the resisting force is dominant, the system becomes stable. Zhao [17] showed the effect of system pressure on natural circulation. He showed, on stability maps, that increasing the system pressure significantly suppresses the instability region in the natural circulation system, especially the intermittent oscillation region. In Fig. 21a, at low pressure the pressure drop of the two phase flow across the riser is high which increases the driving force due to higher density difference, hence why

the oscillations are showing higher amplitude. With further increase in the system pressure, the pump head is reduced and the mass flow rate is increased. The steep pump curve Fig. 7 explains the odd shape of the amplitude curve. It is opposite to the trend in case of natural circulation [15], which experienced a monotonic decrease with the increase of pressure. The incubation time is seen to be reduced with the increase in pressure which is reflected on the time period as shown in Fig. 21b.

5. Conclusions

In this thesis the contribution of the friction and buoyancy forces on the flashing instabilities under forced convection is identified. This experimental study is focused on analysing the wave characteristics under the effect of they pump bypass valve, the system pressure and the heating power. Based on the results, the following is concluded:

1. Three wave forms were observed, namely: irregular intermittent, sinusoidal, and intermittent oscillations. The oscillations were caused by a combination of boiling and flashing. The boiling triggers the oscillations but the onset and condensation of flashing cause the jump in amplitude.
2. Reducing the bypass valve open stabilizes the system, while increasing the heating power and system pressure suppresses the flashing phenomena in forced circulation system. The system is stable when the frictional forces are dominant, which happens at high pressure and/or low power (lower than 50 W).
3. Changing the power alters the oscillations shape, amplitude and frequency. The oscillations amplitude are the highest for low heat flux and low pressure conditions. pressurization at the start-up with a pressure higher than 10 *bar* can avoid the instability zone. The incubation time is reduced monotonically with increase in system pressure.

5.1. Future work

Future developments include installing measuring instruments of pressure and temperature along the riser to have better inspection of the flashing phenomenon. Additionally, a sighting glass in the riser to have image analysis of the phenomenon. Furthermore, the impact of the heater inlet restriction valve on the parameters will be addressed.

References

[1] Masanori Aritomi, Jing Hsien Chiang, Tohru Nakahashi, Masumi Wataru, and Michitsugu Mori. Fundamental study on thermo-hydraulics during start-up in natural circulation boiling water reactors,(i) thermo-hydraulic instabilities. *Journal of Nuclear Science and Technology*, 29(7):631–641, 1992.

[2] World Nuclear Association. Nuclear power in the world today. 2023.

[3] JA Boure, AE Bergles, and L S_ Tong. Review of two-phase flow instability. *Nuclear engineering and design*, 25(2):165–192, 1973.

[4] Ezequiel Manavela Chiapero. Two-phase flow instabilities and flow mal-distribution in parallel channels. 2013.

[5] U.S. Nuclear Regulatory Commission. Lasalle unit 2 loss of recirculation pumps with power oscillation event. Information Notice No. 88-39, 1988.

[6] U.S. Nuclear Regulatory Commission. Power oscillations at washington nuclear power unit 2. Information Notice No. 92-74, 1992.

[7] Kenji Fukuda and Tetsuo Kobori. Classification of two-phase flow instability by density wave oscillation model. *Journal of Nuclear science and Technology*, 16(2):95–108, 1979.

[8] M Furuya, F Inada, and THJJ Van der Hagen. Flashing-induced density wave oscillations in a natural circulation bwr—mechanism of instability and stability map. *Nuclear engineering and design*, 235(15):1557–1569, 2005.

[9] SY Jiang, XX Wu, and YJ Zhang. Experimental study of two-phase flow oscillation in natural circulation. *Nuclear science and engineering*, 135(2):177–189, 2000.

[10] Akshay Kumar Khandelwal and Mamoru Ishii. Two-phase flow instability induced by flashing in natural circulation systems: An analytical approach. *International Journal of Heat and Mass Transfer*, 181:121890, 2021.

[11] A Manera, WJM De Kruijf, THJJ Van der Hagen, and RF Mudde. Experiments with the circus-facility on flashing-induced instabilities during startup of natural-circulation-cooled bwrs. In *Proceedings PHYSOR*, pages 7–11, 2000.

[12] Annalisa Manera and Tim HJJ van der Hagen. Stability of natural-circulation-cooled boiling water reactors during startup: experimental results. *Nuclear technology*, 143(1):77–88, 2003.

[13] Leonardo Carlos Ruspini. Experimental and numerical investigation on two-phase flow instabilities.

[14] Qiang Wang, Puzhen Gao, Xianbing Chen, Zhongyi Wang, and Ying Huang. An investigation on flashing-induced natural circulation instabilities based on relap5 code. *Annals of Nuclear Energy*, 121:210–222, 2018.

[15] Sipeng Wang, Yu-Chen Lin, Guanyi Wang, and Mamoru Ishii. Experimental investigation on flashing-induced flow instability in a natural circulation scaled-down test facility. *Annals of Nuclear Energy*, 171:109023, 2022.

[16] Eugene H Wissler, HS Isbin, and NR Amundson. Oscillatory behavior of a two-phase natural-circulation loop. *AIChE Journal*, 2(2):157–162, 1956.

[17] Yanan Zhao, Minjun Peng, Yifan Xu, and Genglei Xia. Simulation investigation on flashing-induced instabilities in a natural circulation system. *Annals of Nuclear Energy*, 144:107561, 2020.

Abstract in lingua italiana

Gli esperimenti di instabilità del flusso a due fasi sono stati studiati in un circuito a circolazione forzata in condizioni di bassa potenza di riscaldamento e bassa pressione. L'instabilità osservata è stata indotta da flash e le oscillazioni hanno assunto tre forme principali, oscillazione intermittente irregolare, oscillazione sinusoidale pura e oscillazione intermittente. Le caratteristiche delle onde oscillanti sono state analizzate sulla base dei risultati del flusso di massa e della temperatura del fluido. Sono stati inoltre studiati gli effetti della valvola di bypass della pompa, della pressione del sistema e della potenza di riscaldamento sull'ampiezza, la forma e la frequenza delle oscillazioni. Si è riscontrato che il flashing viene soppresso ad alte pressioni e alte potenze, mentre si verificano intense oscillazioni a basso flusso di calore e bassa pressione.

Parole chiave: Circolazione forzata, Lampeggiamento, Instabilità del flusso, Ebollizione